LJMU Research Online

Wang, B, Fielding, AJ and Dryfe, RAW

In situ electrochemical electron paramagnetic resonance spectroscopy as a tool to probe electrical double layer capacitance.

http://researchonline.ljmu.ac.uk/8613/

Article

For more information please contact researchonline@ljmu.ac.uk

http://researchonline.ljmu.ac.uk/

Journal Name

In situ electrochemical electron paramagnetic resonance spectroscopy as a tool to probe electrical double layer capacitance†

Bin Wang,[a] Alistair J. Fielding [b*] and Robert A.W. Dryfe[a*]

Electron paramagnetic resonance (EPR) spectroscopy is applied *in situ* to monitor the electrochemical capacitance of activated carbon in aqueous solutions, thereby revealing aspects of the charge storage mechanism. The EPR signal of activated carbon increases during the charging process and returns reversibly when discharged. Simulation of the spectral lineshape and its temperature dependence indicate that two kinds of spins exist: spin at defects giving rise to a narrow signal, and spins associated with surface-bound aromatic moieties causing a broad signal. A potential-dependent response of the narrow feature is seen in each of the electrolyte solutions used, while changes of the broad feature occur only at higher electrolyte concentrations. The results suggest that the observed increase of unpaired electron density on activated carbon is due to the formation of radical species due to reduction of functional groups. The potential dependence of the broad feature at higher electrolyte concentrations may be related to the further adsorption of ions into the deep porous structure of activated carbon.

Electric double-layer capacitors (EDLCs, also called supercapacitors, SCs) are high power energy storage devices, which depend on the double layer formed at the electrode/electrolyte interface. The classical storage mechanism of EDLCs is the physical adsorption/desorption of ions on the counter-charged pore walls when a potential is applied, and no faradaic reaction is assumed to occur. This physical mechanism ensures a rapid charge/discharge capacity and a long cycle life, which are the defining characteristics of an efficient EDLC.[1] Extensive researches have focused on carbon-based EDLC materials, including activated carbon and samples derived from graphene materials because of their large surface area, tunable pore size and high thermal and chemical stability.[2] The capacitive behaviour has been well-studied by screening different kinds of carbon materials.[2,3,4] A narrow pore system, with pore size below 1.0 nm, has been found to maximize the capacitance.[3] The optimization of the pore structure is used to improve the performance.[4] Even for carbon-based EDLCs, a "pseudo-capacitive" charge storage mechanism, involving Faradaic charge transfer processes, may operate in parallel, notably where oxygen-containing functional groups are present. In recent years, the development of *in situ* techniques (such as the electrochemical quartz crystal microbalance (EQCM),[5] infra-red spectroscopy[6], nuclear magnetic resonance (NMR)[7] and small-angle X-ray or neutron scattering[8]) provides a new molecular-level understanding of this charge-discharge behaviour. The *in situ* EQCM relates the charging process to the magnitude of the adsorbed mass on the electrode.[5] *In situ* NMR gives an intuitive idea about the charging mechanism as "in-pore" ions and solvent molecules can be separated and quantified.[9] Electrochemical electron paramagnetic resonance (EPR) spectroscopy has also been used to study the reduction of carbon materials as localized electron unpaired density can be formed due to the electrochemical process.[10] EPR has the advantage, unlike NMR, infra-red spectroscopy and X-ray photoelectron spectroscopy (XPS), of ready integration with electrochemical cells and detection of paramagnetic sites. The EPR method can therefore be used to detect potential-induced changes in the electrode material, with the wider aim of using such changes to discriminate between purely capacitive and pseudo-capacitive based storage of charge for materials used in supercapacitors.

In this work, an *in situ* EPR cell was designed for use in an aqueous electrolyte, and activated carbon (AC), which is a widely used EDLC material, was chosen as the model material. AC is porous solid carbon, with pore walls formed by graphite nanocrystallites, containing a small number of nanographene layers.[11] The origin of the spin is related to the preparation temperature, as the carbonization process forms localized spins while the graphitization process generates mobile charge

a. *School of Chemistry, University of Manchester, Oxford Road, Manchester, M13 9PL, United Kingdom. E-mail: Robert.dryfe@manchester.ac.uk*

b. *Pharmacy and Biomolecular Science, Liverpool John Moores University, James Parsons Building, Byrom Street, Liverpool, L3 3AF, United Kingdom. E-mail: a.j.fielding@ljmu.ac.uk*

Footnotes relating to the title and/or authors should appear here.

†Electronic Supplementary Information (ESI) available. See DOI: 10.1039/x0xx00000x
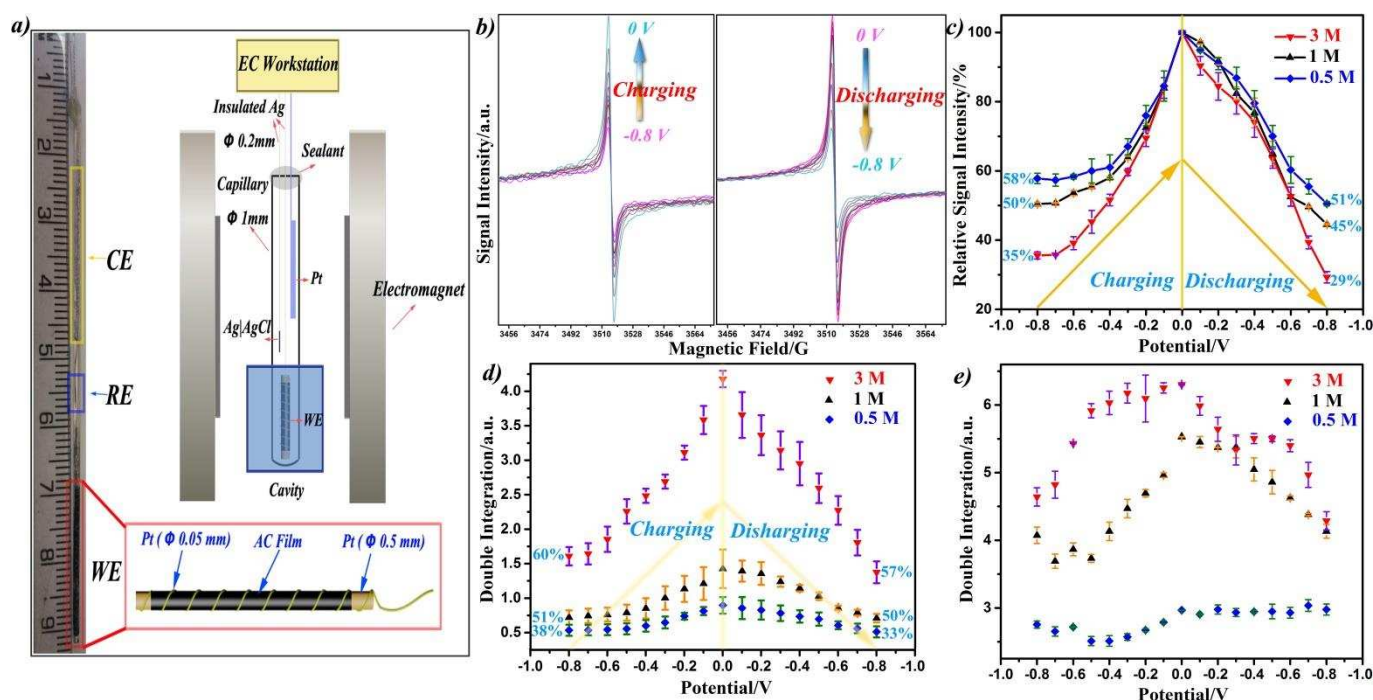
Figure 1. (a) *In situ* EPR cell design: WE represents the AC working electrode, CE denotes the Pt counter electrode and RE the Ag/AgCl reference electrode. (b) The continuous-wave EPR signal change with potential cycling in 3 M KOH. (c) Peak-to-peak intensity change of the EPR signal. (d) Double integration of the narrow component of the EPR signal over charging/discharging different KOH concentrations. (e) Double integration plot, as in (d), applied to the broad component.

carriers.[12] Normally, localized spins obey the Curie law and the spin susceptibility decreases when increasing the temperature. For delocalized electrons, Pauli behavior is anticipated where the spin susceptibility is temperature independent. The *in situ* EPR experiments were carried out by monitoring the spectroscopic signal intensity as a function of electrode potential.

Because pseudo-capacitive storage in carbon materials is primarily related to oxygen-containing functional groups, the oxygen content of our activated carbon samples was assessed via XPS (Figure S1), which suggests a 9 % oxygen composition, associated with hydroxide and carboxylate functionalities. The *in situ* electrochemical EPR cell was based on a three-electrode system as previously used (Figure 1a).[13] The aqueous solution can cause non-resonant absorption of the microwave irradiation causing a weakening the signal.[14] Therefore, a capillary cell was chosen to mitigate against lowering of the cavity Q-factor. The electrochemical performance of the assembled cells is shown in Figure S2a. In all electrolytes, the supported Pt showed a negligible double layer behaviour with the capacitance three orders of magnitude lower than that of active AC electrode (Figure S2b, ESI†). The EPR signal stability of the AC in different electrolytes was also studied and is shown in Figure S2c. The intrinsic signal from the AC was found to decay over time, indicating quenching of radicals. The assembled cell was left for 24 hours before the *in situ* experiment, a procedure which was adopted to reduce the influence from solution. The *in situ* process was monitored over ca. 2 h, during this time the EPR signal variation due to intrinsic decay was very small (< 3 %). The prepared AC-based cell did not give the "classical" rectangular CV curve expected

for an EDLC, which was related to the low conductivity of the prepared AC membrane, the relatively long distance between the electrodes and the limited volume of electrolyte in the capillary.[9c] This work is not, however, pursuing the optimization of capacitance, rather it is focusing on the understanding of the capacitive behaviour by EPR. The EPR signal of AC in electrolyte exhibited an asymmetric shape (A/B=1.16) with a *g* value around 2.0028, similar to previous EPR measurements on AC.[12d,15] The lineshape simulation of AC in electrolyte was found to have two different Lorentzian curves, as shown in Figure S3a. The narrow curve represented the localized spins and the broad component can be attributed to charge carriers or another less localized environment.[16,17] All EPR measurement were made under non-saturating conditions.

The *in situ* electrochemical X band EPR study of the double layer behavior was carried out by applying a potential to the electrode and then monitoring the EPR signal. The Q value during the measurements was assured through use of a ruby standard as described in the ESI†. The capacitive electrode was cycled 20 times to give a stable response (by CV at 20 mV/s, from −0.8 V to 0 V) before the *in situ* EPR study. The EPR signal of AC as a function of potential is shown in Figure 1b and still kept an asymmetric shape with the *g* value of 2.002. As the potential increased from −0.8 V to 0 V, the narrow signal intensity increased and no other peaks were observed. More importantly, this process was reversible; the initial signal intensity was recovered when the potential was cycled back to −0.8 V. On repeating the charging-discharging process for two cycles, the trend of the signal change was highly reproducible. A wide magnetic field scan was also

COMMUNICATION

carried out (Figure S4) and no other peaks were observed. To further interpret the phenomenon shown in Figure 1b, the signal evolution as a function of potential was quantified by the signal intensity and spectral position. Figure 1c displays the peak-to-peak intensity with potential in KOH: the intensity change was triangular, and similar to the charge/discharge curve. The EPR signal of AC at 0 V was the strongest, so the signal was normalized to the response at 0 V. For the charging process, the intensity increased slowly at the beginning, and then increased abruptly up to 0 V. For the discharge process, the EPR signal decreased linearly over the whole voltage range. The g value (Figure S5, ESI†) of the signal, corrected for any drift of microwave frequency, over this potential range fluctuated around 2.0027 when the potential was changed. The peak-to-peak width (Figure S5, ESI†) did not follow a systematic dependence and varied over a small range. All these observations confirmed that the spins observed had similar chemical origin over the potential range sampled.

Supercapacitors store energy in the electrical double layer: i.e. by charge accumulation at the electrode/electrolyte interface. When the cell is charged, a pseudo-capacitive function can arise from groups acting as localised spin traps which accept electrons, forming free radicals. More electrons were localized when the potential increased, due to oxidative transfer of electrons from solution, hence the signal intensity of the narrow component increased with potential. On cell discharge, the density of unpaired electrons was depleted, causing the decrease of EPR signal intensity. As a result, the EPR signal is greatest at 0 V, and is lowest at -0.8 V. Double integration of the narrow curve in Figure 1d confirmed the change of the distribution of spins on AC structure. The change in the *in situ* EPR signal for the narrow component of the AC signal in different KOH concentrations is also studied (Figure 1c,d and Figure S6). The capacitance of AC is limited by the electrolyte (the number of ions at the electrode/electrolyte interface), so the capacitance of AC in 3 M KOH was the greatest (Figure S2a). The smaller capacitance is also reflected in the less extensive charging of sites giving rise to unpaired spins, as reflected in the change of the double integral. The attenuation of the double integration value relative to its maximum value was 62 % during charging in 3 M KOH, and this changed to 40 % in 0.5 M KOH. In addition, the signal strength was related to concentration at each potential, as the EPR intensity of AC in 3 M KOH was the highest (Figure 1d). The broad component was also analysed after Lorentzian line shape simulation (Figure 1e). Interestingly, the potential dependent behaviour of the broad component was not observed in all the electrolytes. For example, the potential dependent behaviour in 3 M KOH was significant (the double integration value change in 3 M KOH was around 2), while a much weaker change occurred in 0.5 M KOH.

In order to study the origin of the spins during charging/discharging, the temperature dependence of the EPR signal from AC for different potentials was studied and is shown in Figure 2. The narrow curve (Figure 2a,b) followed the Curie Law: the double integration value was linear with 1/T, indicating the existence of spins are associated with localised

functional groups.[12d,16] The narrow curve obtained at different potentials always obeyed the Curie Law, indicating that the potential change did not influence the origin of the spin, but only changed their amount. The broad curve (Figure 2c,d) followed a weak Curie Law temperature dependence, indicating that another kind of localized spin existed.[17,18]
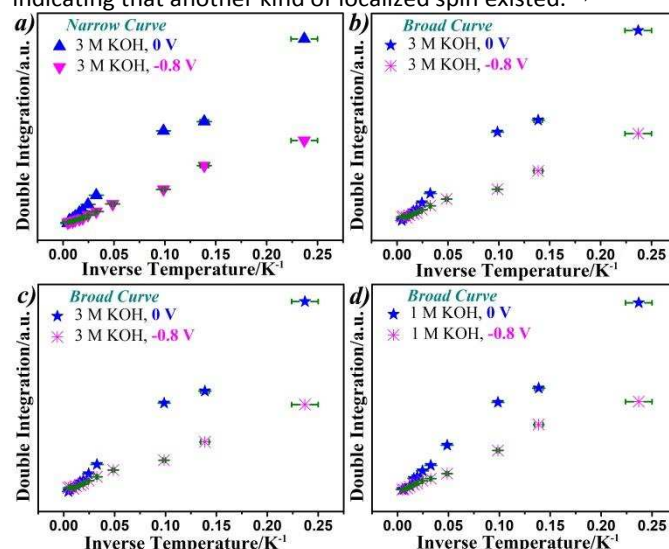

Figure 2. Temperature dependence of EPR behaviour: (a) narrow component and (c) broad component at 0 V at 3 M KOH; (b) narrow component and (d) broad component at 0 V at 1 M KOH. The temperature range was from 4.2 K to 200 K.

Literature suggests that the presence of a broad signal is associated with mobile charge carriers, however, the lack of a Pauli temperature behaviour did not support this.[12d,15] It is possible that the spins from the broad curve are localized on the surface structure on larger, but not extensively delocalised, aromatic units [17], which is consistent with the increased broadening behaviour in the presence of oxygen (Figure S3b).[18] A broad component has been assigned previously to small aromatic units.[17c] Interestingly, the signal change is greatest at 3 M KOH and became much weaker at low concentration KOH (0.5 M). The behaviour of the narrow curve is the most important change in all electrolytes and is likely related to redox chemistry of oxygen-containing functional groups in alkaline electrolyte. The oxidation of carboxylate and alkoxide (e.g. phenoxide) groups form the corresponding radical species, which are consumed gradually during the reduction process. Literature shows that the pseudo-capacitive behaviour of carboxyl and hydroxyl groups is pH dependent as their oxidation is favoured at higher pH.[19] Accordingly, the presence of more functional groups taking part in the redox reaction, and subsequent generation of more localised spins, at higher KOH concentration is consistent with the observed concentration dependence of the *in situ* EPR behavior of AC in KOH electrolytes (Figure 1c,d). The potential dependent behaviour of the broad curve in higher concentration KOH electrolyte may be related to the access of ions into the depths of the porous structure of AC, which provides external capacitance in higher concentration KOH electrolyte. The obvious change of the broad curve and the biggest change of the narrow curve in 3 M KOH electrolyte is consistent with the

highest capacitance of AC in 3 M KOH electrolyte (Figure S2a), showing a strong relationship between the capacitance and the EPR signal change over potential. The open circuit voltage (OCV) of the prepared cell in 1 M KOH was *ca.* −0.3 V vs Ag|AgCl electrode. The EPR signal of AC at the OCV was consistent with the signal without applied potential (Figure S7, ESI†), which lends further support to the proposed correlation between the EPR signal and the applied potential. When the applied potential was interrupted, the EPR signal returned to the initial state (without applied potential or signal at OCV, shown in Figure S7, ESI†). This was because the charge balance on the electrode/electrolyte interface was broken.

Conclusions

In summary, the charging/discharging process of AC was studied by an *in situ* EPR experiment. An increase in the unpaired electron density on activated carbon was seen, yielding an EPR signal at g = 2.0028. This electron density was analysed via its signal intensity and doubly-integrated value. Both EPR signal intensity and the double integration value increased over potential and, then, recovered when the potential returned. The temperature dependent results indicated that the narrow component of the signal was from localized spins at defects, which followed the Curie Law, while the broad component was also from localized spins and attributed to more extended aromatic units. The potential dependent performance of the narrow curve was related to the redox reaction of carboxylic and hydroxyl groups during charging and discharging, when these functional groups are oxidized and, then, consumed on subsequent reduction. The change of the broad curve in higher capacitance electrolyte (1 M and 3 M KOH) may be linked with the access of ions into the depths of the pores of the AC.

Competing interests

The authors declare no competing financial interests.

Acknowledgements

Notes and references

1   a) M. Winter and R. J. Brodd, Chem. Rev., 2004, 104, 4245; (b) A. Burke, J. Power Sources, 2000, 91, 37; (c) J. R. Miller and P. Simon, Science, 2008, 321, 651.
2   (a) G.P. Wang, L. Zhang and J.J. Zhang, Chem. Soc. Rev., 2012, 41, 797-828; (b) L.L. Zhang and X.S. Zhao, Chem. Soc. Rev., 2009, 38, 2520-2531; (c) P. Simon and Y. Gogotis, Acc. Chem. Res., 2013, 46, 1094. (d) G.P. Hao, Q. Zhang, M. Sin,

F. Hippaul, L. Borchardt, E. Bruuner, S. Kaskel, Chem. Mater., 2016, 28, 8715.
3   (a) J. Chmiola, G. Yushin, Y.Gogotsi, C. Portet, P. Simon, P.L. Taberna, Science, 2006, 313, 1760; (b) E. Raymundo-Piñero, K. Kierzek, J. Machnikowski, F. Béguin, Carbon, 2006, 44, 2498.
4   (a) Y. Zhu, S. Murali, M.D. Stoller, K. J. Ganesh, W. Cai, P.J. Ferreira, A. Pirkle and R.S. Ruoff, Science, 2011, 332, 1537-1541; (b) C. Largeot, C. Porter, J. Chmiola, P.L. Taberna, Y.Gogotsi and P. Simon, J. Am. Chem. Soc., 2008, 103, 2730.
5   (a) M.D. Levi, G. Salitra, N. Levy, D. Aurbach, J. Maier, Nat. Mater., 2009, 8, 872; (b) M.D. Levi, N. Levy, S. Sigalov, G. Salitra, N. Levy, D. Aurbach, J. Maier, J. Am. Chem. Soc., 2010, 132, 13220; (c) W.Y. Tsai, P.L. Taberna, P. Simon, J. Am. Chem. Soc., 2014, 136, 8722.
6   (a) F.W. Richey, B. Dyatkin, Y. Gogotsi, Y.A. Elabd, J. Am. Chem. Soc., 2013, 135, 12818; (b) F.W. Richey, C. Tran, V. Kalra, Y.A. Elabd,   J. Phys. Chem. C, 2014, 118, 21846.
7   (a) A.C. Forse, C. Merlet, J.M. Griffin and C.P. Gery, J. Am. Chem. Soc., 2016, 138, 5731; (b) A.J. Ilott, N.M. Trease, C.P. Grey, A. Jerschow, Nat. Commun., 2014, 5, 4536.
8   (a) S. Boukhalfa, D. Gordon, L. He, Y.B. Melnichenko, N. Nitta, A. Magasinski, G. Yushin, ACS Nano, 2014, 8, 2495; (b) S. Boukhalfa, L. He, Y.B. Melnichenko, G. Yushin, Angew. Chem., Int. Ed., 2013, 52, 4618.
9   (a) J.M. Griffin, A.C. Forse, W.Y. Tsai, P.L. Taberna, P. Simon, C.P .Grey, Nat. Mater., 2015, 14, 812; (b) A.C. Forse, J.M. Griffin, C. Merlet, P.M. Bayley, H. Wang, P. Simon, C.P. Grey, J. Am. Chem. Soc., 2015, 137, 7231.
10   (a) J.R. Harbour and M.J. Walzak, Carbon, 1986, 24, 743; (b) J.R. Harbour and M.J. Walzak, Carbon, 1985, 23, 185; (c) J.R. Harbour and M.J. Walzak, Carbon, 1985, 23, 687; (d) J.Tarábeka, L. Kavana, M. Kalbáča, P. Raptaa, M. Zukalováb, L. Dunsch, Carbon, 2006, 44, 2147; (d) H. Maruyama, H. Nakano, M. Nakamoto and A. Sekiguch, Angew. Chem. Int. Ed., 2013, 53, 1324.
11   (a) M. Smisek and S. Cerny, Active Carbon: Manufacture, Properties and Applications (Elsevier, New York, 1967); R. E. Franklin, Proc. Roy. Soc., 1951, A209, 196 (1951); (b) T. Enoki, Phy. Scr., 2012, T146,14008.
12   (a) L.S. Singer, Proceeding of the 5th Conference on Carbon, Pergamon Press, Oxford, 1963, 2, 37; (b) A. Oberline, Carbon, 1984, 22, 521. (c) K. Kawamura, Carbon, 1998, 36, 1227. (d) F.G. Emmerich, Carbon, 1991, 29, 305. (e) L.S. Singer and I.C. Lewis, Appl. Spectrosc., 1982, 36, 52. (f) E. Zhecheva, R. Stoyanova, J.M. Jimenez-Mateos, R. Alcantara, P. Lavela and J.L. Tirado, Carbon, 2002, 40, 2301.
13   J.R. González, R. Alcántara, J.L. Tirado, A.J. Fielding, and R.A.W. Dryfe, Chem. Mater., 2017, 29, 5886.
14   M.A. Tamski, J.V. macpherson, P.R. Unwin and M.E. Newton, Phys. Chem. Chem. Phys., 2015, 17, 23438.
15   S. Łośa, L. Duclaux, W. Kempiński and M. Połomskaa, Micropor. Mesopor. Mat, 2010, 130, 21.
16   (a) A. Więckowski , L. N. Kozdrowska , P. Rechnia , A. Malaika , B. Krzyżyńska and M. Kozłowski, Acta Physica Polonica A, 2016, 130, 701; (b) H. Marsh, F. R. Reinoso, Activated Carbon, Elsevier, Oxford 2006, 31.
17   (a) S. Łoś, M. Letellier, P. Azaïs and L. Duclaux, J. Phys. Chem. Solids, 2006, 67, 1182; (b) T. Enoki and K. Takai, Solid State Commun. 2009, 149, 1144, (c) L.J. Kennedy, J.J. Vijaya and G. Sekaran, Mater. Phys. Chem., 2005, 91, 471.
18   S.J. Boyer and R.B. Clarkson, Colloid Surf. A: Physicochem. Eng. Aspects, 1994, 82, 217.
19   (a) Y.J. Oh, J.Yoo, Y. Kim, J. Yoon, H. Yoon, J. Kim and S.B. Park, Electrochem. Acta, 2014, 116, 118; (b) H.A. Andreas and B.E. Conway, Electrochim. Acta, 2006, 51, 6510.